Inorg. Chem. **2006**, *45*, 9315–9325

Heterobimetallic Zn(II)–Ln(III) Phenylene-Bridged Schiff Base Complexes, Computational Studies, and Evidence for Singlet Energy Transfer as the Main Pathway in the Sensitization of Near-Infrared Nd^{3+} Luminescence

Wing-Kit Lo,[†] Wai-Kwok Wong,*[,†,‡] Wai-Yeung Wong,[†,‡] Jianping Guo,[†] Kai-Tai Yeung,[†] Yuen-Kit Cheng,*[,†] Xiaoping Yang,[†,§] and Richard A. Jones*[,§]

Department of Chemistry and Centre for Advanced Luminescence Materials, Hong Kong Baptist University, Kowloon Tong, Hong Kong, P. R. China, and Department of Chemistry and Biochemistry, The University of Texas at Austin, 1 University Station A5300, Austin, Texas 78712-0165

Received June 7, 2006

A series of 3d–4f heterobimetallic phenylene-bridged Schiff base complexes of the general formula $[Zn(\mu\text{-}L^1)Ln(NO_3)_3(S)_n]$ [Ln = La (**1**), Nd (**2**), Gd (**3**), Er (**4**), Yb (**5**); S = H_2O, EtOH; n = 1, 2; H_2L^1 = *N,N′*-bis(3-methoxysalicylidene)phenylene-1,2-diamine] and $[Zn(\mu\text{-}L^2)Ln(NO_3)_3(H_2O)_n]$ [Ln = La (**6**), Nd (**7**), Gd (**8**), Er (**9**), Yb (**10**); n = 1, 2; H_2L^2 = *N,N′*-bis(3-methoxy-5-*p*-tolylsalicylidene)phenylene-1,2-diamine] were synthesized and characterized. Complexes **1**, **2**, **4**, and **7** were structurally characterized by X-ray crystallography. At room temperature in CH_3CN, both neodymium(III) (**2** and **7**) and ytterbium(III) (**5** and **10**) complexes also exhibited, in addition to the ligand-centered emission in the UV–vis region, their lanthanide(III) ion emission in the near-infrared (NIR) region. The photophysical properties of the zinc(II) phenylene-bridged complexes (ZnL^1 and ZnL^2) were measured and compared with those of the corresponding zinc(II) ethylene-bridged complexes (ZnL^3 and ZnL^4). Our results revealed that, at 77 K, both ligand-centered triplet (^{3}LC) and singlet (^{1}LC) states existed for the ethylene-bridged complexes (ZnL^3 and ZnL^4), whereas only the ^{1}LC state was detected for the phenylene-bridged complexes (ZnL^1 and ZnL^2). NIR sensitization studies of $[Zn(\mu\text{-}L')Nd(NO_3)_3(H_2O)_n]$ (L' = L^1–L^4) complexes further showed that Nd^{3+} sensitization took place via the ^{3}LC and ^{1}LC states when the spacer between the imine groups of the Schiff base ligand was an ethylene and a phenylene unit, respectively. Ab initio calculations show that the observed differences can be attributed to the difference in the molecular vibrational properties and electron densities of the electronic states between the ethylene- and phenylene-bridged complexes.

Introduction

The near-infrared (NIR) photoluminescence (PL) properties of lanthanide(III) ions (Yb^{3+}, Er^{3+}, Nd^{3+}) have been of special interest in recent years because these ions exhibit long luminescence lifetimes and large Stoke's shifts, rendering separation of the luminescence signal from the background fluorescence and scattering relatively easy. Thus, they have found various applications in fluoroimmunoassays, optical amplifiers, and laser devices.[1−3] However, direct excitation of Ln^{3+} ions is difficult because of the weak (Laporte-forbidden) nature of their f−f transitions.[3] One way to overcome this problem is to complex the lanthanide ions by some specifically designed organic sensitizing molecules.[4−7]

* To whom correspondence should be addressed. E-mail: wkwong@hkbu.edu.hk (W.-K.W.). Fax: 852-3411-5862 (W.-K.W.). Tel: 852-3411-7011 (W.-K.W.).

[†] Department of Chemistry, Hong Kong Baptist University.

[‡] Centre for Advanced Luminescence Materials, Hong Kong Baptist University.

[§] Department of Chemistry and Biochemistry, The University of Texas at Austin.

(1) Horrocks, W. D., Jr.; Albin, M. *Progress in Inorganic Chemistry*; Lippard, S. J., Ed.; John Wiley & Sons: New York 1984; Vol. 31, p 1.

(2) *Bioanalytical Applications of Labeling Technologies*; Hemmilä, I., Stählberg, T., Mottram, P., Eds.; Wallac Oy: Turku, Finland, 1994.

(3) Carnall, W. T. *Handbook on the Physics and Chemistry of Rare Earths*; Gschneidner, K. A., Jr., Eyring, L., Eds.; Elsevier: Amsterdam, 1987; Vol. 3, p 171.

(4) Beeby, A.; Dickins, R. S.; Faulkner, S.; Parker, D.; Williams, J. A. G. *Chem. Commun.* **1997**, 1401.

(5) Klink, S. I.; Hebbink, G. A.; Grave, L.; van Veggel, F. C. J. M.; Reinhoudt, D. N.; Slooff, L. H.; Polman, A.; Hofstraat, J. W. *J. Appl. Phys.* **1999**, *86*, 1181.

10.1021/ic0610177 CCC: $33.50
Published on Web 10/17/2006

Chart 1

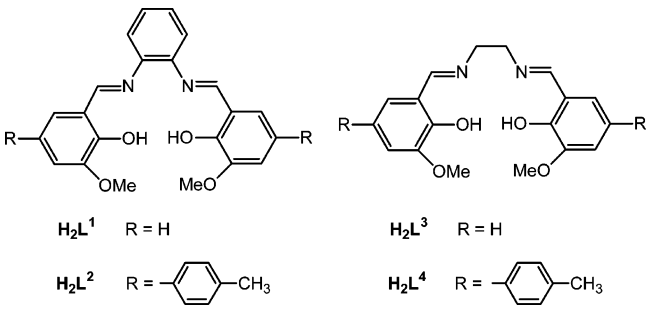

These molecules absorb the excitation energy efficiently, transfer the energy to the lanthanide ion and result in the lanthanide ion luminescence. Therefore, much effort has been devoted to the synthesis of lanthanide complexes with different organic chromophores that can act as coordinating agents and sensitizers dually. Recently, there has been a great interest in using transition metal complexes as tunable low-energy sensitizers for NIR emission from lanthanides.[8] We have shown that zinc(II) Schiff base complexes, which are known to be effective emitters,[9] could act as antenna chromophores for lanthanide(III) ion sensitization.[10] Herein, we report the electronic effect of the substituents and the nature of the spacers (ethylene vs phenylene) of the Schiff base on the PL properties of the resulting zinc(II) and their Zn−4f Schiff base complexes.

Results and Discussion

Preparation of Schiff Base Ligands. The phenylene-bridged Schiff base ligands H_2L^1 and H_2L^2 (Chart 1) were prepared in excellent yield (92%) according to the literature method[10b] via the condensation of 1,2-diaminobenzene with *o*-vanillin and 5-(4′-methylphenyl)-3-methoxysalicylaldehyde, respectively, in a 2:1 mole ratio. The ^{1}H NMR spectrum of H_2L^1 and H_2L^2 in $CDCl_3$ showed a singlet at δ 8.60 and 8.69 for the imino protons and a broad singlet at δ 13.23 and 13.24 for the hydroxyl protons, respectively. The chemical shift of the hydroxyl protons is typical for the resonance-assisted hydrogen-bonded (RAHB) proton of O−H···N=C.[10b,12,13] The crystal structures of H_2L^1 and H_2L^2 depicted in Figures 1 and 2, respectively, revealed the presence of intramolecular hydrogen bonding between the O−H groups and the imino N of the Schiff bases with the N···O distances of 2.563(2) and 2.638(2) Å for H_2L^1 and 2.560(2) and 2.616(2) Å for H_2L^2 and are comparable to those reported for analogous Schiff bases.[10b] The crystal structures further revealed that the inner N_2O_2 cavity of the phenylene-bridged Schiff bases is nonplanar. A similar observation has been reported for the bromo-substituted analogue.[10e] It seems reasonable to assume that this occurs in order to minimize steric interactions between the two phenolic OH protons, which would otherwise be directed to each other. This is due to the repulsion between the two phenolic protons and the repulsion between the two imino nitrogens.

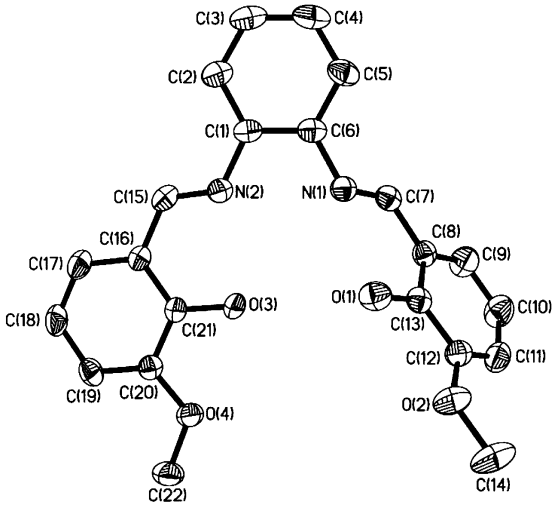

Figure 1. Perspective drawing of H_2L^1.

Preparation of ZnLnL′ Heterobimetallic Complexes. The zinc(II) Schiff base complexes, ZnL′ (L′ = L^1, L^2), were prepared in high yield via the interaction of the free Schiff bases, H_2L', with $Zn(OAc)_2$ in a 1:1 mole ratio in refluxing absolute ethanol for 12 h. Reaction of ZnL′ complexes with 1 equiv of $Ln(NO_3)_3 \cdot xH_2O$ in either refluxing acetonitrile or ethanol gave the heterobimetallic complexes ZnLnL′ of the general formula $[Zn(\mu\text{-}L')Ln(NO_3)_3(S)_n]$ (Ln = La, Nd, Gd, Yb, Er; L′ = L^1, L^2; S = H_2O, EtOH) in high yield (Scheme 1). The ZnLnL′ complexes were easily crystallized out by slow evaporation of their solution in acetonitrile or ethanol. Elemental analyses and FAB MS data supported the formulation. Conductivity measurements showed that com-

(6) (a) Kachura, T. F.; Sevchenko, A. N.; Solov'ev, K. N.; Tsvirko, M. P. *Dokl. Akad. Nauk SSSR* **1974**, *217*, 1211. (b) Gauterman, M.; Schumaker, C. D.; Srivastava, T. S.; Yaneta, T. *Chem. Phys. Lett.* **1976**, *40*, 456.
(7) Beeby, A.; Dickins, R. S.; FitzGerald, S.; Govenlock, L. J.; Maupin, C. L.; Parker, D.; Riehl, J. P.; Siligardi, G.; Williams, J. A. G. *Chem. Commun.* **2000**, 1183.
(8) (a) Klink, S. I.; Keizer, H.; van Veggel, F. C. J. M. *Angew. Chem., Int. Ed.* **2000**, *39*, 4319. (b) Shavaleev, N. M.; Moorcraft, L. P.; Pope, S. J. A.; Bell, Z. R.; Faulkner, S.; Ward, M. D. *Chem. Commun.* **2003**, 1134. (c) Imbert, D.; Cantuel, M.; Bunzli, J.-C. G.; Bernardinelli, G.; Piguet, C. *J. Am. Chem. Soc.* **2003**, *125*, 15698.
(9) Hamada, Y.; Sano, T.; Fujita, M.; Fujii, T.; Nishio, Y.; Shibata, K. *Jpn. J. Appl. Phys.* **1993**, *32*, L511.
(10) (a) Wong, W.-K.; Liang, H.; Wong, W.-Y.; Cai, Z.; Li, K.-F.; Cheah, K.-W. *New J. Chem.* **2002**, *26*, 275. (b) Lo, W.-K.; Wong, W.-K.; Guo, J.-P.; Wong, W.-Y.; Li, K.-F.; Cheah, K.-W. *Inorg. Chim. Acta* **2004**, *357*, 4510. (c) Yang, X.-P.; Jones, R. A.; Lynch, V.; Oye, M. M.; Holmes, A. L. *Dalton Trans.* **2005**, 849. (d) Yang, X.-P.; Jones, R. A. *J. Am. Chem. Soc.* **2005**, *127*, 7686. (e) Yang, X.-P.; Jones, R. A.; Wu, Q.; Oye, M. M.; Lo, W. K.; Wong, W. K.; Holmes, A. L. *Polyhedron* **2006**, *25*, 271.
(11) (a) Costes, J.-P.; Dahan, F.; Dupuis, A. *Inorg. Chem.* **2000**, *39*, 165 and references therein. (b) Costes, J.-P.; Dahan, F.; Dupuis, A.; Laurent, J.-P. *Inorg. Chem.* **2000**, *39*, 169. (c) Costes, J.-P.; Dahan, F.; Dupuis, A. *Inorg. Chem.* **2000**, *39*, 5994. (d) Costes, J.-P.; Dahan, F.; Novitchi, G.; Arion, V.; Shova, S.; Lipkowski, J. *Eur. J. Inorg. Chem.* **2004**, 1530. (e) Novitchi, G.; Shova, S.; Caneschi, A.; Costes, J.-P.; Gdaniec, M.; Stanica, N. *Dalton Trans.* **2004**, 1194. (g) Costes, J.-P.; Dahan, F.; Wernsdorfer, W. *Inorg. Chem.* **2006**, *45*, 5. (g) Costes, J.-P.; Auchel, M.; Dahan, F.; Peyrou, V.; Shova, S.; Wernsdorfer, W. *Inorg. Chem.* **2006**, *45*, 1924. (h) Koner, R.; Lee, G.-H.; Wang, Y.; Wei, H.-H.; Mohanta, S. *Eur. J. Inorg. Chem.* **2005**, 1500.
(12) (a) Gilli, P.; Bertolasi, V.; Ferretti, V.; Gilli, G. *J. Am. Chem. Soc.* **2000**, *124*, 10405. (b) Bertolasi, V.; Gilli, P.; Ferretti, V.; Gilli, G. *J. Am. Chem. Soc.* **1991**, *113*, 4917.

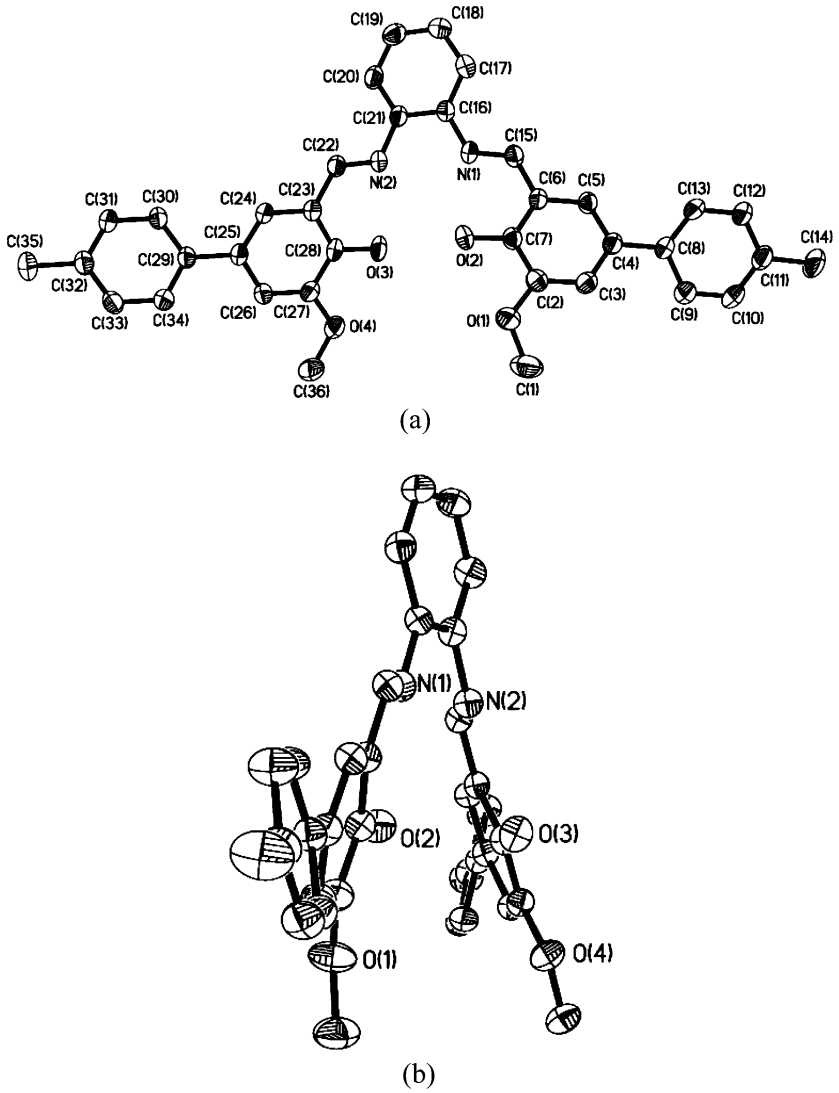

Figure 2. Perspective drawings of H_2L^2: (a) top view; (b) side view.

Scheme 1

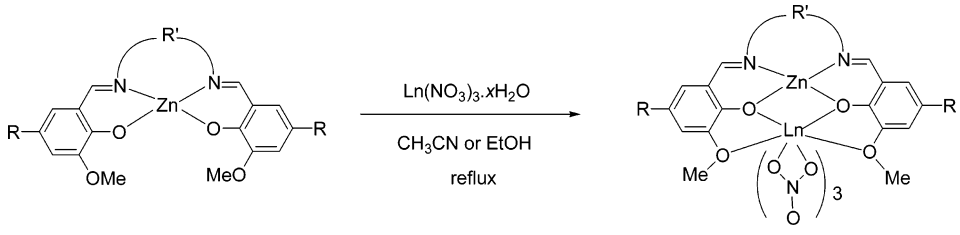

R	R'	ZnL'
H	*o*-C_6H_4	**ZnL^1**
p-tolyl	*o*-C_6H_4	**ZnL^2**
H	CH_2CH_2	**ZnL^3**
p-tolyl	CH_2CH_2	**ZnL^4**

	ZnLnL'			
Ln	L^1	L^2	L^3	L^4
La	**1**	**6**	**11**	**16**
Nd	**2**	**7**	**12**	**17**
Gd	**3**	**8**	**13**	**18**
Er	**4**	**9**	**14**	**19**
Yb	**5**	**10**	**15**	**20**

plexes **1**−**10** behaved as nonelectrolytes and existed as neutral, undissociated species in acetonitrile.

The structures of the heterobimetallic phenylene-bridged Schiff bases complexes **1**, **2**, **4**, and **7** were ascertained by X-ray crystallography, and their perspective drawings are shown in Figures 3−6, respectively, with selected bond distances summarized in Table 1. The structures of the phenylene-bridged complexes are very similar to the corresponding ethylene-bridged[10b] and analogous phenylene-bridged complexes.[10e] Similar structures were also reported

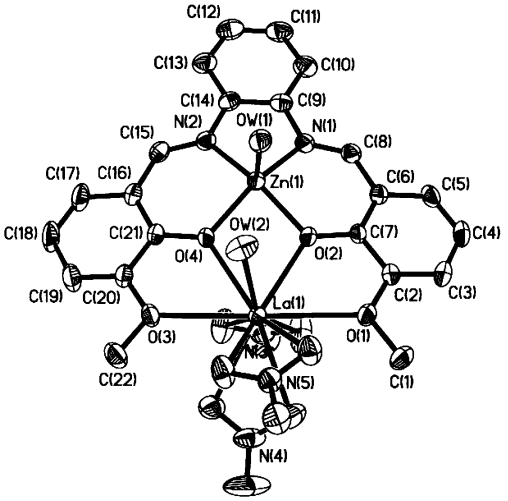

Figure 3. Perspective drawing of compound **1**.

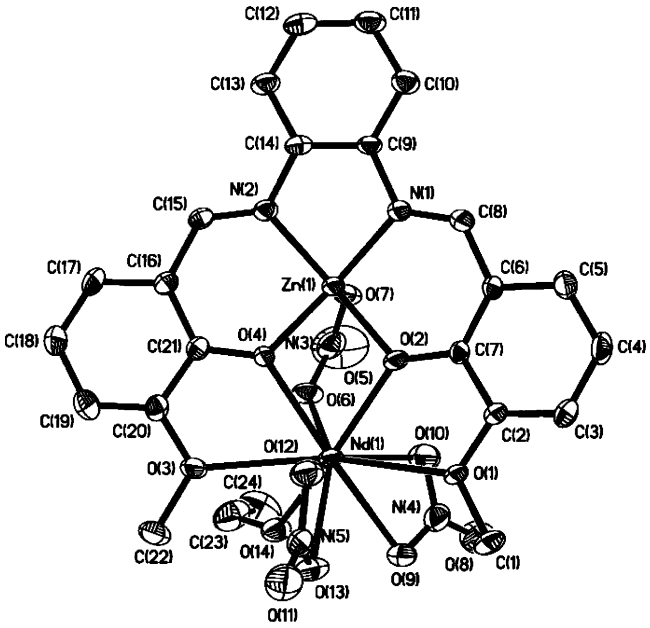

Figure 4. Perspective drawing of compound **2**.

in the pioneering work of Costes and co-workers for related Cu−Gd Schiff base complexes.[11] Structural analyses revealed that the relatively soft transition metal ion, zinc(II), is located in the inner N_2O_2 cavity and the hard lanthanide(III) ion in the outer O_4 cavity of the Schiff base ligand. For the [Zn(μ-L^1)Ln$(NO_3)_3$(S)$_n$] complexes (**1**, Ln = La, S = H_2O, n = 2; **2**, Ln = Nd, S = EtOH, n = 1; **4**, Ln = Er, S = EtOH, n = 1), the zinc(II) ion is five-coordinate and adopts a distorted square pyramidal geometry, with the two imino nitrogen atoms and the two phenolic oxygen atoms forming the square base, while the aqua oxygen (**1**), the bridging nitrato oxygen (**2**), or the monodentate nitrato oxygen (**4**) occupies the axial position. Depending on the size of the Ln^{3+} ions, their coordination number varies from 9 (Er, **4**) and 10 (Nd, **2**) to 11 (La, **1**). The Ln^{3+} ions are surrounded by four O atoms from the Schiff base, two from the bridging phenolic groups and two from the methoxy groups, with the remaining coordination sites by O atoms from aqua (or ethanol) and nitrato ligands. For **1**, the remaining coordination sites are occupied by seven O atoms, six from three

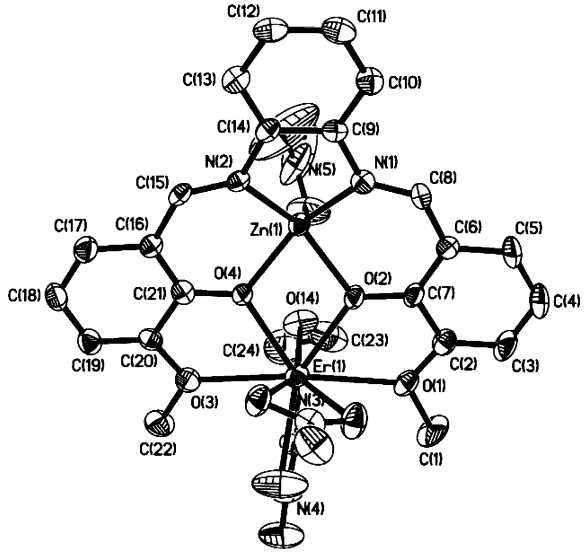

Figure 5. Perspective drawing of compound **4**.

bidentate nitrato ligands and one from the aqua oxygen (Figure 3), for **2**, the sites are occupied by six O atoms, four from two bidentate nitrato ligands, one from bridging nitrato ligand, and one from the ethanol oxygen (Figure 4), and, for **4**, the sites are occupied by five O atoms, four from two bidentate nitrato ligands and one from the ethanol oxygen (Figure 5). The results illustrate that as the ionic size decreases, the lanthanide ion lowers its coordination number to relieve the congestion by converting one of its bidentate nitrato ligand to a sterically less demanding monodentate nitrato ligand. Eventually, the coordination environment of the lanthanide is so congested that it has to transfer the nitrato ligand to the Zn^{2+} ion. Similar observations have been reported for the corresponding ethylene-bridged [Zn(μ-L^4)-Ln$(NO_3)_3(H_2O)_n$] complexes (**16, 17, 19**, **20**).[10b] The structure of **7** (Figure 6) is very similar to that of **2**; the Zn^{2+} and Nd^{3+} ions are also 5- and 10-coordinate, respectively. The only difference is that the axial position of Zn^{2+} ion is occupied by an aqua molecule and the Nd^{3+} ion is coordinated to three bidentate nitrato ligands. The Zn−Ln distances are within 3.387−3.611 Å and are too long for any significant interaction. The average lengths of the Zn−N and Zn−O bonds are in the ranges 2.026−2.034 and 1.992−2.019 Å, respectively, which are comparable to those of other similar zinc(II) Schiff base complexes.[10b,14] The Ln−O average length was in the range 2.403−2.623 Å, which is comparable to those of heterobimetallic 4f−Zn Schiff base complexes.[14b] The decrease in Ln−O distance in the series La^{3+} > Nd^{3+} > Er^{3+} > Yb^{3+} is in agreement with the lanthanide contraction and reflects a decrease in ionic radii: 1.17 > 1.12 > 1.03 > 1.01 Å.[15]

(13) Filarowski, A.; Koll, A.; Glowiak, T. *J. Chem. Soc., Perkin Trans. 2* **2002**, 835.
(14) (a) Connor, J. A.; Charlton, M.; Cupertino, D. C.; Lienke, A.; McPartlin, M.; Scowen, I. J.; Tasker, P. A. *J. Chem. Soc., Dalton Trans.* **1996**, 2835. (b) Raquel, R. C.; Fernando, A.; Carlos, O. L.; Daniel, I.; Bunzli, J.-C. G.; Andres de, B.; Teresa, R. B. *Inorg. Chem.* **2002**, *41*, 5336.
(15) Cotton, F. A.; Wilkinson, G.; Murillo, C. A.; Bochmann, M. *Advanced Inorganic Chemistry*, 6th ed.; John Wiley & Sons: New York, 1999; p 1109.

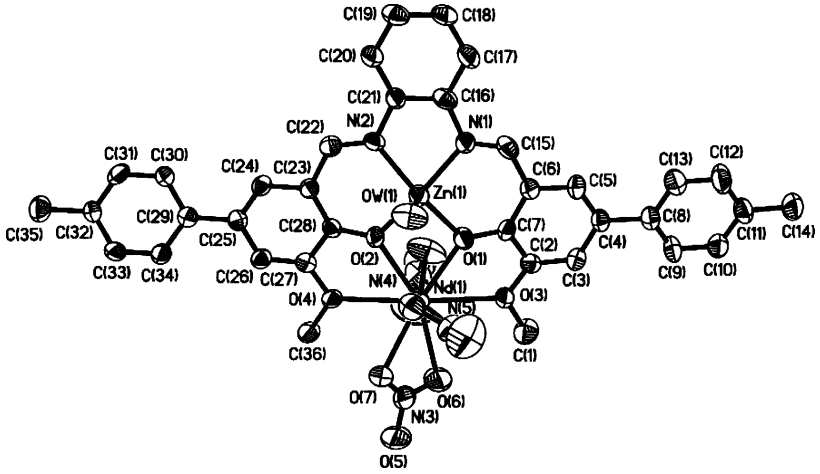

Figure 6. Perspective drawing of compound **7**.

Table 1. Selected Bond Distances (Å) of ZnLnL′ Complexes

param	**1** (ZnLaL[1])	**2** (ZnNdL[1])	**4** (ZnErL[1])	**7** (ZnNdL[2])
Zn−N(1)	2.027(2)	2.034(7)	2.033(6)	2.022(5)
Zn−N(2)	2.027(2)	2.029(7)	2.035(5)	2.030(5)
av Zn−N	2.027	2.032	2.034	2.026
Zn−O(2)	2.007(19)	2.011(5)	2.030(4)	2.011(5)
Zn−O(4)	1.977(19)	2.008(5)	2.008(4)	1.989(5)
av Zn−O	1.992	2.010	2.019	2.000
Ln−O(1)	2.764(18)	2.749(5)	2.547(5)	2.389(4)
Ln−O(2)	2.489(19)	2.382(5)	2.255(5)	2.423(4)
Ln−O(3)	2.722(19)	2.728(6)	2.535(5)	2.627(5)
Ln−O(4)	2.517(18)	2.453(5)	2.273(4)	2.688(4)
av Ln−O	2.623	2.578	2.403	2.532
Zn···Ln	3.611	3.387	3.463	3.506

Photophysical Properties of ZnL′ and ZnLnL′. The photophysical properties of ZnL′ (L′ = L[1]−L[4]) complexes have been examined, and the data are summarized in Table 2. The room temperature (RT) solution electronic absorption, excitation, and emission spectra of ZnL′ complexes in the UV−vis region are very similar and are characteristic of intraligand transitions of Schiff base complexes. The absorption between 240 and 380 nm can be assigned to the $\pi \rightarrow \pi^*$ transitions of the Schiff base ligands. The RT emission of ZnL′ complexes, with lifetimes (τ) ranging from 0.63 to 1.10 ns and quantum yields (Φ_{em}) of $(0.34-15.09) \times 10^{-3}$, can be assigned to the intraligand singlet state emission. The photophysical properties of the Schiff base complexes can be fine-tuned by changing the linkage between the two Schiff base units or the electronic properties of the substituents on the flanking phenyl rings. By extension of the conjugation either through the spacer or substituents, the absorption and emission spectra of the complexes are red shifted. For instance, by replacement of a *p*-H with a *p*-tolyl group (ZnL[1] vs ZnL[2] or ZnL[3] vs ZnL[4]), the absorption and emission maxima of the complexes are red shifted by about 20 nm. The effect is even more pronounced with variation of the spacer. When the spacer was changed from an ethylene to a phenylene bridge, the emission maximum is red shifted by about 60 nm (480 to 540 nm for ZnL[3] vs ZnL[1]; 500 to 565 nm for ZnL[4] vs ZnL[2]). However, the quantum yield of the ethylene-bridged complexes is much higher than the corresponding phenylene-bridged complexes. This may be due to the fact that phenylene-bridged complexes show a stronger nonradiative relaxation through internal conversion (IC) or intersystem crossing (ISC) followed by vibrational relaxation, which quenches the emission, than the corresponding ethylene-bridged complexes.

At 77 K, the ethylene-bridged complexes (ZnL[3] and ZnL[4]) exhibit both ligand-centered singlet (^{1}LC) and triplet (^{3}LC) emission, whereas the phenylene-bridged complexes (ZnL[1] and ZnL[2]) exhibit only ^{1}LC emission. Figure 7a shows the absorption, emission and excitation spectra of ZnL[4]. The RT excitation spectrum of ZnL[4] (monitored at 500 nm) is identical with its 77 K excitation spectrum (monitored at 520 nm) indicating that both emissions come from the same origin. Time-resolved spectra and lifetime measurements showed that both ^{1}LC fluorescence (470 nm, τ = 4.93 ns) and ^{3}LC phosphorescence (520 nm, τ = 7.77 ms) coexisted at 77 K. ^{3}LC emission was not observed at RT even in an oxygen-free solvent system. Figure 7b shows the absorption, emission, and excitation spectra of ZnL[2]. The emission peak is blue shifted by 20 nm as the temperature is lowered to 77 K. The RT excitation spectrum of ZnL[2] (monitored at 565 nm) is identical with its 77 K excitation spectrum (monitored at 545 nm). The time-resolved spectrum and lifetime measurement showed that the emission at 545 nm (τ = 2.77 ns) corresponds to ^{1}LC fluorescence. ^{3}LC phosphorescence was not observed even at 77 K. Ab initio calculations show that the observed differences can be attributed to the difference in the molecular vibrational properties and electron densities of the electronic states between the ethylene- and phenylene-bridged complexes (vide infra).

The photophysical properties of ZnLnL′ complexes (**1**−**20**) have been examined, and selected data are summarized in Table 3. At RT, the absorption and emission spectra of ZnLnL′ in the UV−vis region are similar to those of the corresponding ZnL′ complexes, being blue shifted by 15−20 nm as compared to those complexes. The UV−vis absorption ranging from 410 to 266 nm and emission with lifetimes (τ) ranging from 0.82 to 4.60 ns can be assigned to the $\pi \rightarrow \pi^*$ transitions and intraligand emission of the Schiff base ligands, respectively. In addition to the visible emission, all the ZnLnL′ complexes (Ln = Nd, Er, Yb), except compounds **4** and **9**, exhibit emission corresponding to the Ln^{3+} ion in the NIR region. For the ZnNdL′

Table 2. Photophysical Data of ZnL′ Complexes[a]

compd	abs: λ_{max}/nm [log(ϵ/dm^3 mol^{-1} cm^{-1})]	excitatn: λ_{ex}/nm	emission at 298 K: λ_{em}/nm (τ, $10^3\Phi_{em}$)[b]	emission at 77 K: λ_{em}/nm (τ)	$S_1 \rightarrow S_0$:[c] calcd (nm)	$T_1 \rightarrow S_0$:[c] calcd (nm)
ZnL^1	417 (4.19), 312 (4.41) 258 (4.44)	413, 333	540 (0.69 ns, 0.55)	507 (2.36 ns)	564 (463)	840 (675)
ZnL^2	441 (4.15), 311 (4.83)	355	565 (0.63 ns, 0.34)	545 (2.77 ns)	569 (455)	826 (690)
ZnL^3	368 (3.89), 283 (4.15)	368, 284	480 (1.10 ns, 15.09)	449 (7.78 ns) 494 (44.99 ms)	438 (365)	638 (553)
ZnL^4	385 (4.02), 311 (4.70) 279 (4.84)	383, 313	500 (0.86 ns, 14.24)	470 (4.93 ns) 520 (7.77 ms)	447 (365)	651 (567)

[a] Measurements were done in 1×10^{-5} M solution in DMSO. [b] Quantum yield was measured relative to quinine sulfate in 1.0 N H_2SO_4 ($\Phi_{em} = 0.55$). [c] Assuming Franck−Condon vertical emissions, corresponding adiabatic values are given in parentheses. $S_1 \rightarrow S_0$ emission values are based on TD-DFT calculations.

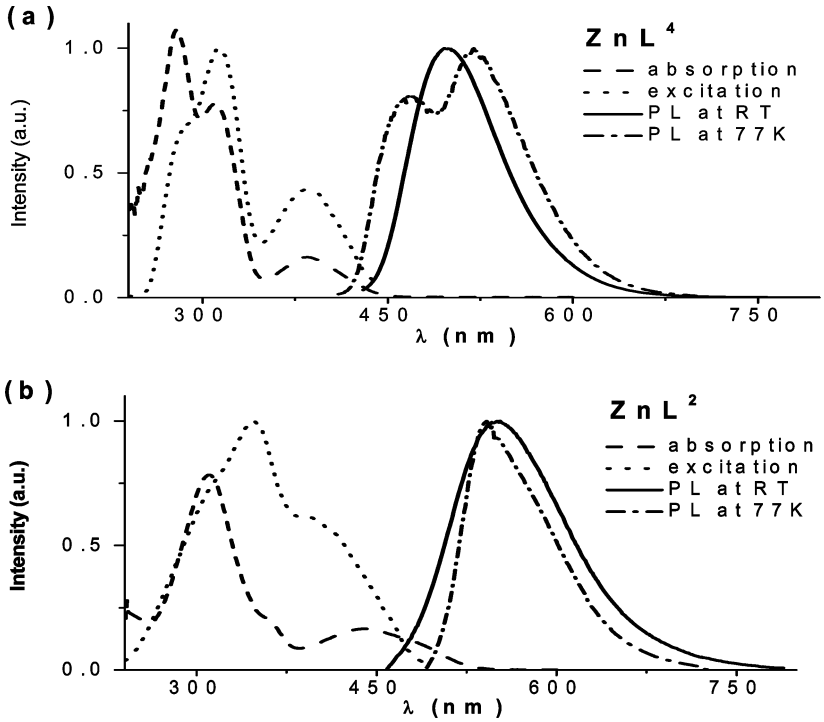

Figure 7. Absorption, excitation (monitored at 500 nm), and emission spectra of (a) ZnL^4 and (b) ZnL^2 in DMSO.

complexes, the emissions at 875, 1068, and 1356 nm can be assigned to $^4F_{3/2} \rightarrow {}^4I_{9/2}$, $^4F_{3/2} \rightarrow {}^4I_{11/2}$, and $^4F_{3/2} \rightarrow {}^4I_{13/2}$ transitions of Nd^{3+}, respectively. For the ZnErL′ and ZnYbL′ complexes, the emissions at 1515 and 976 nm can be assigned to the $^4I_{13/2} \rightarrow {}^4I_{15/2}$ transition of Er^{3+} and $^2F_{5/2} \rightarrow {}^2F_{7/2}$ transition of Yb^{3+}, respectively. These NIR emissions are very similar to those reported for Nd^{3+}, Er^{3+}, and Yb^{3+}, and the lifetime values are in good agreement with literature values.[16a,17] Figure 8 shows the NIR emission spectra of ZnNdL′ complexes (**2**, **7**, **12**, and **17**). The excitation spectra of **2**, **7**, **12**, and **17** monitored at the NIR emission peak (875 nm) are similar to that monitored at the visible emission peak. This clearly shows that both visible and NIR emissions are originated from the $\pi \rightarrow \pi^*$ transitions of the Schiff base ligands. The emission spectra and decay time measurements for Gd^{3+} complexes allowed the identification of the lowest ligand triplet state (T_1) in the complexes.[16] Earlier studies showed that, for the ethylene-bridged ZnGdL^4 complex (**18**), both LC singlet and triplet states were detected at 77 K; for ethylene-bridged complexes ZnLnL^3 and ZnLnL^4 (Ln = Nd, Er, Yb), NIR sensitization of Ln^{3+} proceeds via the T_1 state of the ethylene-bridged Schiff base ligand.[10b] However, for the phenylene-bridged Gd^{3+} complexes (**3** and **8**), only the ^{1}LC but no ^{3}LC state was observed even at 77 K. Figure 9 shows the absorption, excitation, and emission spectra of **8**. Time-resolved spectra showed that the emission at both RT and 77 K corresponds to ^{1}LC emission with lifetime being 1.58 and 3.85 ns, respectively. The results indicate that, for complexes **3** and **8**, the T_1 state of the phenylene-bridged Schiff base ligand is nonemissive and probably decays via vibrational relaxation. For the ethylene-bridged complexes ZnLnL^3 and ZnLnL^4 (Ln = Nd, Er, Yb), the NIR emission intensity for Er^{3+} is rather weak and is at least 1 order of magnitude weaker than the corresponding Nd^{3+} and Yb^{3+}.[10a,b]

(16) (a) Klink, S. I.; Grave, L.; Reinhoudt, D. N.; van Veggel, F. C. J. M.; Werts, M. H.; Geurts, F. A. J.; Hofstraat, J. W. *J. Phys. Chem. A* **2000**, *104*, 5457. (b) de Sá, G. F.; Malta, O. L.; de Mello Donegai, C.; Simas, A. M.; Longo, R. L.; Santa-Cruz, P. A.; da Silva, E. F., Jr. *Coord. Chem. Rev.* **2000**, *196*, 165. (c) Kawamura, Y.; Wada, Y.; Yanagida, S. *Jpn. J. Appl. Phys.* **2001**, *40*, 350.

(17) (a) Shavaleev, N. M.; Pope, S. J. A.; Bell, Z. R.; Faulkner, S.; Ward, M. D. *Dalton Trans.* **2003**, 808 and references therein. (b) Hebbink, G. A.; Reinhoud, D. N.; van Veggel, F. C. J. M. *Eur. J. Org. Chem.* **2001**, 4101. (c) Klink, S. I.; Hebbink, G. A.; Grave, L.; Peters, F. G. A.; van Veggel, F. C. J. M.; Reinhoud, D. N.; Hofstraat, J. W. *Eur. J. Org. Chem.* **2000**, 1923. (d) Werts, M. H. V.; Verhoeven, J. W.; Hofstraat, J. W. *J. Chem. Soc., Perkin Trans. 2* **2000**, 433.

Table 3. Photophysical Data for ZnLnL′[a] Complexes (**1**−**20**)[b] in CH_3CN

complex	abs, λ_{max}/nm [log(ϵ/dm^3 mol^{-1} cm^{-1})]	excitatn: λ_{ex}/nm	emission at 298 K: λ_{em}/nm (τ, $10^3\Phi_{em}$)[c]	emission at 77 K: λ_{em}/nm (τ)
1	330 (4.18), 301 (4.35)	360	518 (0.91 ns, 2.8×10^{-2})	
2	330 (4.20), 301 (4.37)	360	496 (1.12 ns, $<10^{-2}$) 875 (1.23 μs)[d]	
3	330 (4.25), 301 (4.33)	379, 336	518 (1.56 ns, $<10^{-2}$)	509 (2.97 ns)
4	330 (4.28), 303 (4.38)	360	515 (1.87 ns, $<10^{-2}$)	
5	330 (4.30), 303 (4.45)	380	509 (1.41 ns, $<10^{-2}$) 976 (13.40 μs)	
6	410 (3.88), 336 (4.32), 284 (4.66)	400, 348	551 (0.81 ns, 2.4×10^{-2})	
7	410 (3.96), 336 (4.45), 283 (4.77)	400, 352, 308	545 (1.65 ns, $<10^{-2}$) 875 (1.27 μs)	
8	410 (3.84), 336 (4.30), 280 (4.65)	413, 338, 296	551 (1.58 ns, $<10^{-2}$)	536 (3.85 ns)
9	410 (3.87), 336 (4.31), 280 (4.69)	394, 343, 302	546 (2.00 ns, $<10^{-2}$)	
10	410 (3.86), 336 (4.33), 280 (4.67)	395, 348, 308	545 (1.00 ns, $<10^{-2}$) 976 (15.89 μs)	
11	345 (3.84), 266 (4.27)	355, 299	476 (4.22 ns, 0.97)	441 (4.61 ns) 485 (8.97 ms)
12	346 (3.88), 266 (4.29)	345, 276	465 (1.16 ns, $<10^{-2}$) 875 (1.32 μs)	
13	340 (3.82), 266 (4.24)	347, 276	460 (0.82 ns, 0.65)	460 (7.65 ns) 498 (8.62 ms)
14	340 (3.87), 265 (4.29)	347, 279	460 (1.16 ns, 0.16) 1515[e]	
15	344 (3.85), 267 (4.26)	350, 277	470 (1.09 ns, 0.13) 976 (11.26 μs)	
16	362 (3.90), 270 (4.87)	355, 300	480 (1.90 ns, 2.17)	457 (4.09 ns) 515 (3.53 ms)
17	362 (3.83), 271 (4.81)	372, 305	480 (4.60 ns, $<10^{-2}$) 875 (1.30 μs)	
18	362 (3.99), 269 (4.91)	365, 280	480 (1.90 ns, 0.38)	455 (2.11 ns) 515 (6.10 ms)
19	360 (3.77), 267 (4.76)	365, 300	480 (4.30 ns, $<10^{-2}$) 1515	
20	366 (3.75), 267 (4.73)	370, 300	480 (4.30 ns, $<10^{-2}$) 976 (14.59 μs)	

[a] Measurements were done in 1×10^{-5} M solution in CH_3CN. [b] Data for compounds **12**, **14**, and **15** were taken from ref 9a, and data for compounds **16**−**20** were from ref 9b. [c] Quantum yield was measured relative to quinine sulfate in 1.0 N H_2SO_4 ($\Phi_{em} = 0.55$). [d] Due to the limitations of the instrument, we were unable to determine the quantum yield of the NIR luminescence. [e] Due to the limitations of the instrument, we were unable to measure the lifetime of the NIR luminescence of Er^{3+} compounds.

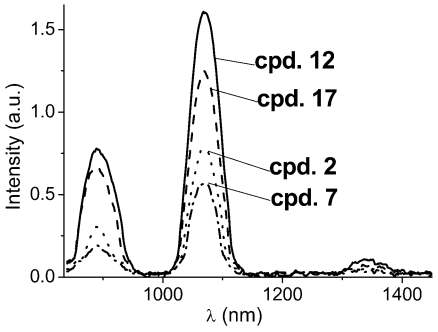

Figure 8. Room-temperature Nd^{3+} emission of different ZnNdL′ Schiff base complexes in CH_3CN upon excitation at 355 nm.

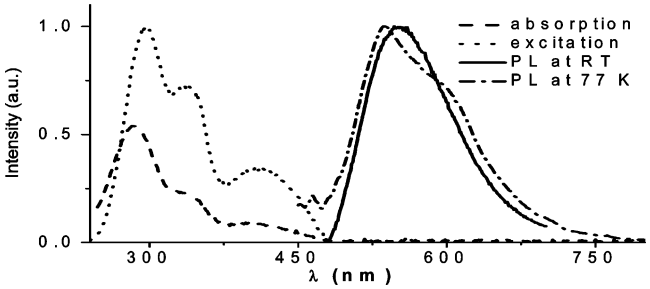

Figure 9. Absorption, excitation (monitored at 500 nm), and emission spectra of **8** in CH_3CN.

The intrinsic quantum yield of Ln^{3+} emission (Φ_{Ln}) may be estimated by $\Phi_{Ln} = \tau_{obs}/\tau_0$, where τ_{obs} is the observed emission lifetime and τ_0 is the "natural lifetime", viz. 14, 2, and 0.25 ms for Er^{3+}, Yb^{3+}, and Nd^{3+}, respectively.[16a] Due to the limitation of our instrument, we were unable to determine τ_{obs} for Er^{3+} and thus could not estimate Φ_{Ln} for Er^{3+}. However, our observation is consistent with literature data that Φ_{Ln} for Er^{3+} is much lower than that of Yb^{3+} and Nd^{3+}.[16a,17] Unlike the ethylene-bridged complexes, we were unable to observe the NIR emission of Er^{3+} for the phenylene-bridged complexes ZnErL[1] and ZnErL[2]. This may due to the fact that the quantum yield of ZnL′ complexes is much higher for the ethylene-bridged than the corresponding phenylene-bridged Schiff base complexes (vide supra). A combination of the above two factors (low Φ_{Ln} of Er^{3+} and low $\Phi_{ZnL'}$) renders the NIR emission of Er^{3+} too weak to be observed for the phenylene-bridged compounds **4** and **9**.

Computational Studies. Computational methods are given in the Experimental Section. Complexes were all modeled with a Zn-coordinated crystallographically observed water molecule (see Figure 3). Since the T_1 states of the phenylene-bridged complexes were computed using density functional theory (DFT) which already considers electron correlation, no time-dependent density functional theory (TD-DFT) $T_1 \rightarrow S_0$ calculations for these complexes were performed.

For the $S_1 \rightarrow S_0$ transitions, the computed values (Table 2) corroborate the observed red shifts caused by the phen-

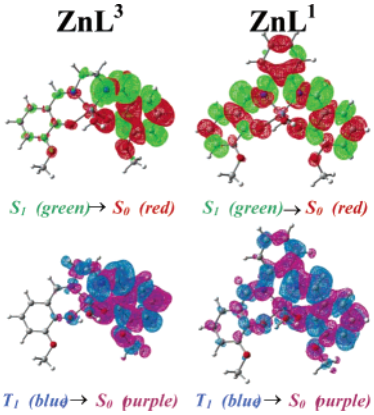

Figure 10. Electron density difference plots (4×10^{-4} e au^{-3}) between the S_1/T_1 and S_0 states of ZnL^1 and ZnL^3. (Electron densities move from the green area for S_1 to the red area for S_0 and from the blue area for T_1 to the purple area for S_0.) Plots are based on the DFT/PBE0/3-21G*-optimized geometry of T_1 for the $T_1 \rightarrow S_0$ transition and the CIS/3-21G*-optimized geometry of S_1 for the $S_1 \rightarrow S_0$ transition.

ylene bridge (ZnL^1 and ZnL^2 vs ZnL^3 and ZnL^4, respectively), and all are within 53 nm of the experimental values. TD-DFT was used to improve the known poor performance of energetic predictions (severe overestimates) based on configuration interaction with single excitation (CIS) optimized geometries alone.[18] The total electron density difference between the excited and the ground states (Figure 10) reveals the extensive delocalization for the $\pi \rightarrow \pi^*$ transitions found in the phenylene-bridged complex ZnL^1 which is in sharp contrast to the laterally localized nature of the ethylene-bridged counterpart ZnL^3. The phenylene bridge also draws electron density toward the bond between the imino nitrogen atoms and the carbon bridge, which maintain the electronic and mechanical couplings of the whole ligand across the bridge in the S_1 states. In view of the small differences (ca. 50−60 kcal/mol) between the zero order energies of the S_1 and S_0 states for ZnL′, Franck−Condon factor (FCF) controlled radiationless IC may still be operative if effective vibrational relaxations coupled to the environment exist. In fact, according to the normal modes analysis on the S_1 states, simulated spectra (see Figure S1, Suppporting Information) of the phenylene-bridged complex ZnL^1 (aided by visual inspection of the individual modes) indicate low-frequency whole-ligand vibrations being dominated in contrast to the more back and forth lateral vibrations with respect to the metal center in the ethylene-bridged complex ZnL^3. This might explain the relatively strong fluorescence quenching of the phenylene-bridged complexes ZnL^1 and ZnL^2 (Table 3). The latter two complexes can efficiently dissipate the excess energy from IC through low-frequency whole-molecule vibrational collisions with the solvent continuum. Instead, calculated ground-state S_0 normal modes (not shown) for *all* the complexes are dominated by whole-skeletal vibrations as also found in the S_1 states of the phenylene-bridged complexes.

For the $T_1 \rightarrow S_0$ transitions, the severe overestimated emission wavelengths (Table 2) are well-known and attributed to the high-density low-lying triplet states and possibly metal−ligand charge transfer (MLCT). In fact, slight MLCT was predicted (Figure 10). ZnL^4 was correctly predicted to phosphoresce at a longer wavelength than ZnL^3, and the unobserved phosphorescence of ZnL^1 and ZnL^2 was estimated to be significantly longer. The absence of phosphorescence in the phenylene-bridged complexes points to ineffective $S_1 \rightarrow T_1$ ISC. Distinctive electronic redistributions in the phenylene bridge of ZnL^1 were calculated in the T_1 state with respect to the S_1 state (Figure 10), and the distribution was also asymmetrically distorted. This will diminish the FCF-controlled ISC. As in the S_1 cases, the normal mode vibrations of the T_1-state phenylene-bridged complexes again involve the whole-molecule small-amplitude motions, in contrast to the relatively large asymmetric movement around the metal center found in the ethylene-bridged complexes. Thus, spin−orbit coupling (SOC) also disfavors ISC in the phenylene-bridged complexes as a result for which vibrational motions around the heavy metal atom are small. Taken together, the unobserved phosphorescence in the phenylene-bridged complexes is rationalized as ineffective SOC and FCF-controlled $S_1 \rightarrow T_1$ ISC, which has an important implication in the molecular design of Schiff base photosensitization via ^{3}LC state. Previous work by Güdel et. al. focused on ligand-to-metal energy transfer mechanisms and rates in ligand−lanthanide complexes as a whole and did not focus on structural differences in the ligands.[19] In contrast our computations focus on the specific design of the ligand bridge (ethylene vs phenylene) for the Zn-coordinated ligands (without the lanthanide) in facilitating or impeding ^{1}LC or ^{3}LC sensitization in the final lanthanide complexes.

In conclusion, we have demonstrated, that due to the difference in vibrational properties and electronic configurations, ZnL′ complexes exhibited both ^{1}LC and ^{3}LC emissions with ethylene-bridged ligands but only ^{1}LC emission with phenylene bridges at 77 K. For the ZnNdL′ complexes, Nd^{3+} sensitization was via the ^{3}LC state with ethylene-bridged complexes and most likely via the ^{1}LC state with phenylene-bridged complexes.

Experimental Section

Materials and Instruments. Solvents and starting materials were all purchased commercially and used without further purification unless otherwise stated. 5-(4′-Methylphenyl)-3-methoxysalicylaldehyde was prepared according to literature method.[10b] Elemental analyses (C, H, N) were performed by the Shanghai Institute of Organic Chemistry, Chinese Academy of Sciences, Shanghai, P. R. China. Electronic absorption spectra in the UV−vis region were recorded on a Hewlett-Packard 8453 UV−visible spectrophotometer, steady-state visible fluorescence and PL excitation spectra, on a Photon Technology International (PTI) Alphascan spectrofluorometer, and visible decay spectra, on a pico-N_2 laser system (PTI Time Master) with $\lambda_{ex} = 337$ nm. Quantum yields of visible emissions were computed according to the literature method[20] using

(18) Halls, M. D.; Schlegal, H. B. *Chem. Mater.* **2001**, *13*, 2632.

(19) (a) Reinhard, C.; Güdel, H. U. *Inorg. Chem.* **2002**, *41*, 1048. (b) Gonçalves e Silva, F. R.; Malta, O. L.; Reinhard, C.; Güdel, H. U.; Piguet, C.; Moser, J. E.; Bünzli, J.-C. G. *J. Phys. Chem. A* **2002**, *106*, 1670.

(20) Parker, C. A.; Rees, W. T. *Analyst (London)* **1960**, *85*, 587.

quinine sulfate in 0.1 N H_2SO_4 as the reference standard (Φ = 0.55 in air-equilibrated water).[21] NIR emission was detected by a liquid-nitrogen-cooled InSb IR detector (EG & G) with a preamplifier and recorded by a lock-in amplifier system. The third harmonics, 355 nm line of a Nd:YAG laser (Quantel Brilliant B), was used as the excitation light source. The emission spectra have been corrected for the spectral response of the instrument. Infrared spectra (KBr pellets) were recorded on a Nicolet Nagna-IR 550 spectrometer, and NMR spectra, on a JEOL EX270 spectrometer. Chemical shifts of ^{1}H and ^{13}C NMR spectra were referenced to internal deuterated solvents and then recalculated to $SiMe_4$ (δ 0.00). Low-resolution mass spectra (LRMS) were obtained on a Finnegan MAT SSQ-710 spectrometer in the positive FAB mode. Electrospray ionization high-resolution mass spectra (ESI−HRMS) were recorded on a QSTAR mass spectrometer. Conductivity measurements were carried out with a DDS-11 conductivity bridge for 10^{-4} mol dm^{-1} solutions in CH_3CN.

Preparation of Schiff Base Ligands. Phenylene-bridged Schiff base ligands H_2L^1 and H_2L^2 were synthesized using the same procedures as for the ethylene-bridged Schiff bases H_2L^3 and H_2L^4.[10b] A typical procedure is given for H_2L^1.

Preparation of H_2L^1. *o*-Vanillin (3.35 g, 22.0 mmol) was added to a solution of 1,2-diaminobenzene (1.08 g, 10.0 mmol) in absolute ethanol (50 mL). The resulting mixture was stirred and refluxed overnight. After being cooled to RT, the orange crystalline product precipitated out, and the product was washed with cold ethanol and petroleum ether. The crude product was redissolved in $CHCl_3$ and evaporated to dryness to furnish H_2L^1 as an orange solid. Yield: 3.58 g (95%), mp 166−168 °C. ^{1}H NMR ($CDCl_3$): δ 13.23 (s, 2H, O*H*), 8.60 (s, 2H, *H*C═N), 7.32−7.30 (m, 2H, Ar*H*), 7.19−7.17 (m, 2H, Ar*H*), 7.00−6.94 (m, 4H, Ar*H*), 6.86−6.82 (m, 2H, Ar*H*), 3.88 (s, 6H, OCH_3). ^{13}C NMR ($CDCl_3$): δ 164.12, 151.44, 148.39, 142.34, 127.53, 123.79, 120.14, 119.02, 118.41, 114.83, 55.99. MS (FAB, +ve): *m*/*z* 377 [M + 1]$^+$. UV−vis ($CHCl_3$, 20 °C) {λ_{max}/nm [log(ϵ/dm^3 mol^{-1} cm^{-1})]}: 336 (4.26), 281 (4.46), 239 (4.43). Fluorescence ($CHCl_3$, 20 °C): λ_{ex}/nm, 398, 326, 303; λ_{em}/nm, 480. IR (cm^{-1}, KBr): 3451 m, 1613 s, 1569 m, 1469 s, 1257 s, 1205 s, 1073 m, 972 s, 781 m, 742 s.

Preparation of H_2L^2. 5-(4′-Methylphenyl)-3-methoxysalicylaldehyde (0.51 g, 2.10 mmol) and 1,2-diaminobenzene (0.11 g, 1.00 mmol) were used. A red solid of H_2L^2 was obtained. Yield: 0.53 g (95%), mp198−200 °C. ^{1}H NMR ($CDCl_3$): δ 13.24 (s, 2H, OH), 8.69 (s, 2H, HC═N), 7.47−7.45 (m, 4H, ArH), 7.37−7.35 (m, 2H, ArH), 7.26−7.23 (m, 6H, ArH), 7.20−7.18 (m, 4H, ArH), 3.95 (s, 6H, OCH_3), 2.39 (s, 6H, $ArCH_3$). ^{13}C NMR ($CDCl_3$): δ 164.31, 150.98, 147.78, 142.39, 137.72, 136.72, 132.03, 129.50, 127.66, 126.58, 122.05, 120.30, 119.12, 114.24, 56.28, 21.05. UV−vis ($CHCl_3$, 20 °C) {λ_{max}/nm [log(ϵ/dm^3 mol^{-1} cm^{-1})]}: 335 (4.34), 272 (4.83). Fluorescence ($CHCl_3$, 20 °C): λ_{ex}/nm, 335, 304; λ_{em}/nm, 496. MS (FAB, +ve): *m*/*z* 557 [M + H]$^+$. IR (cm^{-1}, KBr): 2928 m, 1616 s, 1581 s, 1515 m, 1464 s, 1450 m, 1270 s, 1120 s, 1115 m, 985 m, 810 s, 747 s.

Preparation of Zinc(II) Schiff Base Complexes ZnL′. Zinc(II) phenylene-bridged Schiff bases ZnL^1 and ZnL^2 complexes were synthesized using the same procedures as for the zinc(II) ethylene-bridged Schiff bases ZnL^3 and ZnL.[410b] A typical procedure is given for ZnL^1.

Synthesis of ZnL^1. To a stirred suspension of H_2L^1 (4.21 g, 11.17 mmol) in absolute ethanol (30 mL) was added $Zn(OAc)_2\cdot 2H_2O$ (2.70 g, 12.29 mmol), and the reaction mixture was heated under reflux overnight. The insoluble yellow precipitate was filtered out, washed with ethanol and $CHCl_3$, and dried under vacuum. ZnL^1 was isolated as an orange solid. Yield: 4.318 g (88%), mp > 300 °C. ^{1}H NMR (DMSO-d_6): δ 9.01 (s, 2H, *H*C═N), 7.91−7.84 (m, 2H, Ar*H*), 7.39−7.36 (m, 2H, Ar*H*), 7.03 (d, *J* = 7.6 Hz, 2H, Ar*H*), 6.86 (d, *J* = 7.6 Hz, 2H, Ar*H*), 6.44 (t, *J* = 7.6 Hz, 2H, Ar*H*), 3.77 (s, 6H, OCH_3). MS (FAB, +ve): *m*/*z* 439 [M + H]$^+$. IR (cm^{-1}, KBr): 3318 m, 1613 s, 1586 s, 1540 s, 1467 s, 1444 s, 1388 m, 1237 s, 1193 s, 1106 m, 975 m, 737 s.

Synthesis of ZnL^2. H_2L^2 (0.12 g, 0.22 mmol) and $Zn(OAc)_2\cdot 2H_2O$ (0.05 g, 0.24 mmol) were used. An orange solid of ZnL^2 was obtained. Yield: 0.125 g (92%), mp > 300 °C. ^{1}H NMR (DMSO-D_6): δ 9.15 (s, 2H, *H*C═N), 7.95−7.92 (m, 2H, Ar*H*), 7.57 (d, *J* = 8.1 Hz, 4H, Ar*H*), 7.42 (bs, 4H, Ar*H*), 7.23 (d, *J* = 8.1 Hz, 4H, Ar*H*), 7.18 (bs, 2H, Ar*H*), 3.87 (s, 6H, OCH_3), and 2.33 (s, 6H, *p*-$C_6H_4CH_3$). MS (FAB, +ve): *m*/*z* 619 [M + H]$^+$. IR (cm^{-1}, KBr): 3368 m, 1615 s, 1584 s, 1538 m, 1515 m, 1463 s, 1274 m, 1194 s, 980 m, 814 m, 742 m.

Preparation of ZnLnL′ Complexes. Heterobimetallic Schiff base complexes ZnLnL′ of the general formula [Zn(μ-L′)Ln$(NO_3)_3$-$(S)_n$] (Ln = La, Nd, Gd, Er, Yb; L′ = L^1−L;[4] S = H_2O, EtOH; *n* = 1, 2) were prepared via the reaction of ZnL′ with an equimolar amount of $Ln(NO_3)_3\cdot xH_2O$ in refluxing acetonitrile or ethanol. Ethylene-bridged complexes **12** and **14**−**20** have been reported earlier.[10b] The same procedures were used for the preparation of complexes **11** and **13** and the phenylene-bridged complexes (**1**−**10**). A typical procedure is given for complex **1**.

Synthesis of [Zn(μ-L^1)La$(NO_3)_3(H_2O)_2$] (1). When $La(NO_3)_3\cdot 6H_2O$ (0.070 g, 0.162 mmol) was added to a suspension of ZnL^1 (0.065 g, 0.148 mmol) in ethanol at refluxing temperature, a clear pale yellow color was observed. The solution was refluxed for 12 h, cooled to RT, and then filtered. The filtrate, when allowed to evaporate slowly at RT, gave yellow crystals of **1** in about 1 week. Yield: 0.085 g (75%), mp > 300 °C. MS (FAB, +ve): *m*/*z* 701 [Zn(μ-L^1)La$(NO_3)_2$]$^+$ for ^{64}Zn and ^{138}La. IR (cm^{-1}, KBr): 3423 m, 1618 s, 1503 s, 1458 s, 1384 s, 1354 m, 1322 m, 1237 s, 1195 s, 962 m, 735. Anal. Calcd (found) for $C_{22}H_{22}N_5O_{15}ZnLa$ (*M* = 800.72): C, 32.99 (33.35); H, 2.77 (2.68); N, 8.74 (8.84).

Synthesis of [Zn(μ-L^1)Nd$(NO_3)_3$(EtOH)] (2). $Nd(NO_3)_3\cdot 6H_2O$ (0.068 g, 0.12 mmol) and ZnL^1 (0.062 g, 0.141 mmol) were reacted in refluxing ethanol. Yellow crystals of **2** were obtained. Yield: 0.081 g (75%), mp > 300 °C. MS (FAB, +ve): *m*/*z* 707 [Zn(μ-L^1)Nd$(NO_3)_2$]$^+$ for ^{64}Zn and ^{144}Nd. IR (cm^{-1}, KBr): 3423 m, 1613 s, 1586 m, 1549 m, 1457 m, 1384 s, 1302 m, 1235 m, 1194 m, 964 m, 742 m. Anal. Calcd (found) for $C_{24}H_{24}N_5O_{14}ZnNd$ (*M* = 816.09): C, 35.32 (35.10); H, 2.96 (2.72); N, 8.58 (8.92).

Synthesis of [Zn(μ-L^1)Gd$(NO_3)_3$(EtOH)] (3). $Gd(NO_3)_3\cdot 6H_2O$ (0.062 g, 0.137 mmol) and ZnL^1 (0.055 g, 0.125 mmol) were reacted in refluxing ethanol. Yellow crystals of **3** were obtained. Yield: 0.069 g (70%), mp > 300 °C. MS (FAB, +ve): *m*/*z* 720 [Zn(μ-L^1)Gd$(NO_3)_2$]$^+$ for ^{64}Zn and ^{157}Gd. IR (cm^{-1}, KBr): 3423 m, 1612 s, 1586 s, 1550 m, 1528 m, 1468 s, 1384 s, 1302 m, 1235 s, 1193 s, 1027 m, 856 m, 741 m. Anal. Calcd (found) for $C_{24}H_{24}N_5O_{14}ZnGd$ (*M* = 829.07): C, 34.77 (33.98); H, 2.92 (2.47); N, 8.44 (8.84).

Synthesis of [Zn(μ-L^1)Er$(NO_3)_3$(EtOH)] (4). $Er(NO_3)_3\cdot 5H_2O$ (0.057 g, 0.129 mmol) and ZnL^1 (0.051 g, 0.116 mmol) were reacted in refluxing ethanol. Yellow crystals of **4** were obtained. Yield: 0.060 g (65%), mp > 300 °C. MS (FAB, +ve): *m*/*z* 731 [Zn(μ-L^1)Er$(NO_3)_2$]$^+$ for ^{64}Zn and ^{167}Er. IR (cm^{-1}, KBr): 3405 m, 1613 s, 1585 m, 1549 m, 1470 s, 1384 s, 1286 s, 1233 m, 1193 s, 1031 m, 964 m, 745 m. Anal. Calcd (found) for $C_{24}H_{24}N_5O_{14}ZnEr$ (*M* = 839.11): C, 34.35 (34.17); H, 2.88 (2.80); N, 8.34 (8.41).

(21) Meech, S. R.; Phillips, D. C. *J. Photochem.* **1983**, *23*, 193.

Table 4. Crystal Data and Structural and Refinement

param	H_2L^1	H_2L^2	**1** ($ZnLaL^1$)	**2** ($ZnNdL^1$)	**4** ($ZnErL^1$)	**7** ($ZnNdL^2$)
formula	$C_{22}H_{20}N_2O_4$	$C_{36}H_{32}N_2O_4$	$C_{22}H_{22}N_5O_{15}ZnLa$	$C_{24}H_{24}N_5O_{14}ZnNd$	$C_{24}H_{24}N_5O_{14}ZnEr$	$C_{38}H_{35}N_6O_{14}ZnNd$
formula mass	376.40	556.64	800.72	816.09	839.11	1009.33
cryst system	monoclinic	monoclinic	monoclinic	triclinic	monoclinic	orthorhombic
space group	$P2_1/c$	$P2_1/n$	$P2_12_12_1$	$P\bar{1}$	$P2_1/c$	$Fdd2$
a/Å	6.6523(8)	16.7610(18)	13.7989(9)	9.5729(11)	15.9057(13)	50.377(3)
b/Å	16.879(2)	7.4221(8)	14.1239(9)	12.5568(15)	9.1628(8)	16.4194(9)
c/Å	17.184(2)	23.799(3)	14.3394(9)	13.7143(16)	20.5282(17)	19.3599(10)
α/deg	90	90	90	86.346(2)	90	90
β/deg	97.910(2)	105.982(2)	90	73.593(2)	106.688(2)	90
γ/deg	90	90	90	67.874(2)	90	90
V/Å^3	1911.1(4)	2846.2(5)	2794.7(3)	1463.3(3)	2865.8(4)	16013.7(15)
F_{000}	792	1176	1568	810	1652	8032
Z	4	4	4	2	4	16
D_{calcd}/mg m^{-3}	1.308	1.299	1.894	1.852	1.945	1.666
μ/mm^{-1}	0.091	0.085	2.449	2.652	3.825	1.957
θ range for data/deg	1.70−25.99	1.73−27.51	2.02−28.27	1.55−27.53	1.34−28.29	1.68−27.54
tot. reflcns	10 181	16 015	16 657	8757	16 383	23 224
unique reflcns	3734	6372	6463	6354	6597	7746
R_{int}	0.0297	0.0514	0.0201	0.0406	0.0526	0.0568
obsd reflcns [$I > 2\sigma(I)$]	2009	3023	6126	3564	3461	4563
final R indices [$I > 2\sigma(I)$]	R1 = 0.0393	R1 = 0.0517	R1 = 0.0201	R1 = 0.0557	R1 = 0.0446	R1 = 0.0383
	wR2 = 0.0983	wR2 = 0.1237	wR2 = 0.0524	wR2 = 0.1248	wR2 = 0.0911	wR2 = 0.0717
final R indices (all data)	R1 = 0.0882	R1 = 0.1234	R1 = 0.0225	R1 = 0.1145	R1 = 0.1214	R1 = 0.0897
	wR2 = 0.1165	wR2 = 0.1515	wR2 = 0.0535	wR2 = 0.1545	wR2 = 0.1165	wR2 = 0.0835

Synthesis of [Zn(μ-L^1)Yb(NO$_3$)$_3$(H$_2$O)] (5). $Yb(NO_3)_3{\cdot}5H_2O$ (0.067 g, 0.149 mmol) and ZnL^1 (0.060 g, 0.136 mmol) were reacted in refluxing ethanol. Yellow crystals of **5** were obtained. Yield: 0.071 g (65%), mp > 300 °C. MS (FAB, +ve): *m*/*z* 736 $[Zn(\mu\text{-}L^1)Yb(NO_3)_2]^+$ for ^{64}Zn and ^{173}Yb. IR (cm^{-1}, KBr): 3423 m, 1613 s, 1586 m, 1467 s, 1384 s, 1284 s, 1233 m, 1194 s, 964 m, 747 m. Anal. Calcd (found) for $C_{22}H_{20}N_5O_{14}ZnYb$ (M = 816.81): C, 32.35 (32.39); H, 2.47 (2.52); N, 8.57 (8.60).

Synthesis of [Zn(μ-L^2)La(NO$_3$)$_3$(H$_2$O)$_2$] (6). $La(NO_3)_3{\cdot}6H_2O$ (0.024 g, 0.055 mmol) and ZnL^2 (0.030 g, 0.048 mmol) were reacted in refluxing CH_3CN. Yellow crystals of **6** were obtained. Yield: 0.034 g (75%), mp > 300 °C. ^{1}H NMR (CD_3CN): δ 9.13 (s, 2H, *H*C=**N), 7.93 (bs, 2H, Ar***H*), 7.60−7.57 (m, 8H, Ar*H*), 7.51 (bs, 2H, Ar*H*), 7.32 (bs, 2H, Ar*H*), 7.29 (bs, 2H, Ar*H*), 4.19 (s, 6H, OC*H*$_3$) and 2.39 (s, 6H, *p*-$C_6H_4CH_3$). MS (FAB, +ve): *m*/*z* 882 $[Zn(\mu\text{-}L^2)La(NO_3)_2]^+$ for ^{64}Zn and ^{138}La. IR (cm^{-1}, KBr): 3421 m, 1616 s, 1550 m, 1459 s, 1384 s, 1306 m, 1264 m, 1186 m, 1094 m, 980 m, 814 m. Anal. Calcd (found) for $C_{36}H_{34}N_5O_{15}ZnLa$ (M = 980.99): C, 44.08 (43.96); H, 3.49 (3.52); N, 7.14 (7.08).

Synthesis of [Zn(μ-L^2)Nd(NO$_3$)$_3$(H$_2$O)] (7). $Nd(NO_3)_3{\cdot}6H_2O$ (0.026 g, 0.059 mmol) and ZnL^2 (0.032 g, 0.052 mmol) were reacted in refluxing CH_3CN. Yellow crystals of **7** were obtained. Yield 0.042 g (85%), mp > 300 °C. MS (FAB, +ve): *m*/*z* 887 $[Zn(\mu\text{-}L^2)Nd(NO_3)_2]^+$ for ^{64}Zn and ^{144}Nd. IR (cm^{-1}, KBr): 3420 m, 1616 s, 1586 m, 1555 m, 1464 s, 1384 s, 1264 m, 1186 m, 1094 m, 820 m. Anal. Calcd (found) for $C_{36}H_{32}N_5O_{14}ZnNd{\cdot}CH_3CN$ (M = 1009.33): C, 45.22 (45.11); H, 3.50 (3.56); N, 8.33 (8.28).

Synthesis of [Zn(μ-L^2)Gd(NO$_3$)$_3$(H$_2$O)] (8). $Gd(NO_3)_3{\cdot}6H_2O$ (0.028 g, 0.062 mmol) and ZnL^2 (0.035 g, 0.056 mmol) were reacted in refluxing CH_3CN. Yellow crystals of **8** were obtained. Yield: 0.044 g (82%), mp > 300 °C. MS (FAB, +ve): *m*/*z* 900 $[Zn(\mu\text{-}L^2)Gd(NO_3)_2]^+$ for ^{64}Zn and ^{157}Gd. IR (cm^{-1}, KBr): 3419 m, 1616 s, 1586 m, 1551 m, 1516 m, 1466 s, 1384 s, 1305 m, 1265 m, 1185 m, 1094 m, 970 m, 814 m. Anal. Calcd (found) for $C_{36}H_{32}N_5O_{14}ZnGd$ (M = 981.31): C, 44.06 (44.38); H, 3.29 (3.56); N, 7.17 (7.08).

Synthesis of [Zn(μ-L^2)Er(NO$_3$)$_3$(H$_2$O)] (9). $Er(NO_3)_3{\cdot}5H_2O$ (0.037 g, 0.083 mmol) and ZnL^2 (0.045 g, 0.075 mmol) were reacted in refluxing CH_3CN. Yellow crystals of **9** were obtained. Yield: 0.058 g (79%), mp > 300 °C. MS (FAB, +ve): *m*/*z* 908 $[Zn(\mu\text{-}L^2)Er(NO_3)_2]^+$ for ^{64}Zn and ^{167}Er. IR (cm^{-1}, KBr): 3446 m, 1616 s, 1551 m, 1518 s, 1477 s, 1385 s, 1265 s, 1185 m, 1079 m, 985 m, 829 m. Anal. Calcd (found) for $C_{36}H_{32}N_5O_{14}ZnEr$ (M = 991.31): C, 43.62 (43.48); H, 3.25 (3.34); N, 7.06 (7.01).

Synthesis of [Zn(μ-L^2)Yb(NO$_3$)$_3$(H$_2$O)] (10). $Yb(NO_3)_3{\cdot}5H_2O$ (0.025 g, 0.056 mmol) and ZnL^2 (0.031 g, 0.050 mmol) were reacted in refluxing CH_3CN. Yellow crystals of **10** were obtained. Yield: 0.041 g (84%), mp > 300 °C. MS (FAB, +ve): *m*/*z* 915 $[Zn(\mu\text{-}L^2)Yb(NO_3)_2]^+$ for ^{64}Zn and ^{173}Yb. IR (cm^{-1}, KBr): 3421 m, 1616 m, 1477 m, 1384 s, 1306 m, 1265 m, 1187 m, 1115 m, 814 m. Anal. Calcd (found) for $C_{36}H_{32}N_5O_{14}ZnYb$ (M = 997.09): C, 43.36 (43.28); H, 3.24 (3.25); N, 7.02 (7.00).

Synthesis of [Zn(μ-L^3)La(NO$_3$)$_3$(H$_2$O)$_2$] (11). $La(NO_3)_3{\cdot}6H_2O$ (0.292 g, 0.674 mmol) and ZnL^3 (0.240 g, 0.613 mmol) were reacted in refluxing CH_3CN. Yellow crystals of **11** were obtained. Yield: 0.405 g (90%), mp > 300 °C. ^{1}H NMR (CD_3CN): δ 8.53 (s, 2H, *H*C=**N), 7.15 (dd,** J = 1.4 Hz, J = 8.1 Hz, 2H, Ar*H*), 7.08 (dd, J = 1.4 Hz, J = 8.1 Hz, 2H, Ar*H*), 6.82 (t, J = 8.1 Hz, 2H, Ar*H*) and 4.01 (s, 6H, OC*H*$_3$) and 3.92 (s, 4H, −NC*H*$_2$C*H*$_2$N−). MS (FAB, +ve): *m*/*z* 652 $[Zn(\mu\text{-}L^3)La(NO_3)_2]^+$ for ^{64}Zn and ^{138}La. IR (cm^{-1}, KBr): 3423 m, 1641 s, 1456 s, 1384 s, 1309 m, 1282 m, 1219 s, 1073 m, 1034 m, 955 m, 849 s, 736 m, 639 m. Anal. Calcd (found) for $C_{18}H_{22}N_5O_{15}ZnLa$ (M = 752.69): C, 28.72 (28.46); H, 2.95 (3.04); N, 9.30 (9.14).

Synthesis of [Zn(μ-L^3)Gd(NO$_3$)$_3$(H$_2$O)] (13). $Gd(NO_3)_3{\cdot}6H_2O$ (0.291 g, 0.645 mmol) and ZnL^3 (0.230 g, 0.587 mmol) were reacted in refluxing CH_3CN. Yellow crystals of **13** were obtained. Yield: 0.371 g (84%), mp > 300 °C. MS (FAB, +ve): *m*/*z* 673 $[Zn(\mu\text{-}L^3)Gd(NO_3)_2]^+$ for ^{64}Zn and ^{157}Gd. IR (cm^{-1}, KBr): 3372 m, 1635 s, 1457 s, 1385 m, 1344 m, 1281 m, 1220 m, 1168 m, 1074 m, 1030 m, 966 s, 856 s, 785 m, 737 s, 639 m. Anal. Calcd (found) for $C_{18}H_{20}N_5O_{14}ZnGd$ (M = 753.02): C, 28.71 (28.58); H, 2.68 (2.71); N, 9.30 (9.18).

X-ray Crystallography. Pertinent crystallographic data and other experimental details are summarized in Table 4. Single crystals suitable for X-ray diffraction studies were grown by slow evaporation of the respective sample solution in air: H_2L^1 and H_2L^2 from a chloroform/petroleum ether mixture; compounds **1**, **2**, and **4** from an ethanol solution; compound **7** from an acetonitrile solution. The

selected crystal was mounted on the top of a glass fiber for data collection. Intensity data were collected at 293 K on a Bruker Axs SMART 1000 CCD area-detector diffractometer using graphite-monochromated Mo Kα radiation ($\lambda = 0.710\ 73$ Å). The collected frames were processed with the software SAINT,[22] and an absorption correction was applied (SADABS)[23] to the collected reflections. The structures of all compounds were solved by direct methods (SHELXTL)[24] and refined against F^2 by full matrix least-squares analysis. All non-hydrogen atoms were refined anisotropically for these structures. Hydrogen atoms were generated in their idealized positions and allowed to ride on their respective parent carbon atoms.

Computational Methods. For all the singlet ground electronic state (S_0) and the first excited triplet state (T_1), geometry optimizations were performed at the DFT level using the 3-21G* basis set. The PBE0 hybrid functional[25,26] was used based on parameter-free combining of the PBE generalized gradient approximation functional[27] with predefined amount of HF exchange. Vibrational normal modes and $T_1 \rightarrow S_0$ transition energies were then computed using the optimized geometries. To obtain information for the first excited singlet state (S_1), geometry optimizations and the subsequent calculations on vibrational normal modes were also carried out at the configuration interaction with single excitation (CIS)[28] level with the 3-21G* basis set. Electronic transition energies between S_1 and S_0 were calculated on the basis of the difference between the HF energies of S_0 computed separately and the CIS energies of S_1. To obtain more accurate prediction of the $S_1 \rightarrow S_0$ vertical transition energies including some account of electron correlation, time-dependent density functional theory (TD-DFT)[29−32] using PBE0 functional with 3-21G* basis set was applied at the CIS-optimized geometries for the $S_1 \rightarrow S_0$ transition. All the HF, DFT, and TD-DFT calculations were performed using Gaussian 03 (revisions B.05),[33] while the CIS calculations were performed by Gaussian 98 (revisions A.11).[34] Complexes were all modeled with a Zn-coordinated crystallographically observed water molecule (see Figure 1). Since the T_1 states of the phenylene-bridged complexes were computed using DFT which already considers electron correlation, no TD-DFT $T_1 \rightarrow S_0$ calculations for these complexes were performed.

Acknowledgment. We thank the Hong Kong Baptist University (Grant FRG/03-04/II-52), the Hong Kong Research Grants Council (Grant HKBU 2038/02P), and the Robert A. Welch Foundation (Grant F-816) for financial support.

Supporting Information Available: X-ray crystallographic data as a CIF file. This material is available free of charge via the Internet at http://pubs.acs.org.

IC0610177

(22) *SAINT, Reference Manual*; Siemens Energy and Automation: Madison, WI, 1994−1996.
(23) Sheldrick, G. M. *SADABS, Empirical Absorption Correction Program*; University of Göttingen: Göttingen, Germany, 1997.
(24) Sheldrick, G. M. *SHELXTL, Reference Manual*, ver. 5.1; Siemens Energy and Automation: Madison, WI, 1997.
(25) Perdew, J. P.; Ernserhof, M.; Burke, K. *J. Chem. Phys.* **1996**, *105*, 9982.
(26) Adamo, C.; Barone, V. *J. Chem. Phys.* **1999**, *110*, 6158.
(27) Perdew, J. P.; Ernserhof, M.; Burke, K. *Phys. Rev. Lett.* **1996**, *77*, 3865.
(28) Foresman, J. B.; Head-Gordon, M.; Pople, J. A.; Frisch, M. J. *J. Phys. Chem.* **1992**, *96*, 135.
(29) Runge, E.; Gross, E. K. U. *Phys. Rev. Lett.* **1984**, *52*, 997.
(30) Petersilka, M.; Grossmann, U. J.; Gross, E. K. U. *Phys. Rev. Lett.* **1996**, *76*, 1212.
(31) Jamorski, C.; Casida, M. E.; Salahub, D. R. *J. Chem. Phys.* **1996**, *104*, 5134.
(32) Casida, M. E. In *Recent Advances in Density Functional Methods, Part I*; Chong, D. P., Ed.; World Scientific: Singapore, 1995.
(33) Frisch, M. J.; Trucks, G. W.; Schlegel, H. B.; Scuseria, G. E.; Robb, M. A.; Cheeseman, J. R.; Montgomery, J. A., Jr.; Vreven, T.; Kudin, K. N.; Burant, J. C.; Millam, J. M.; Iyengar, S. S.; Tomasi, J.; Barone, V.; Mennucci, B.; Cossi, M.; Scalmani, G.; Rega, N.; Petersson, G. A.; Nakatsuji, H.; Hada, M.; Ehara, M.; Toyota, K.; Fukuda, R.; Hasegawa, J.; Ishida, M.; Nakajima, T.; Honda, Y.; Kitao, O.; Nakai, H.; Klene, M.; Li, X.; Knox, J. E.; Hratchian, H. P.; Cross, J. B.; Adamo, C.; Jaramillo, J.; Gomperts, R.; Stratmann, R. E.; Yazyev, O.; Austin, A. J.; Cammi, R.; Pomelli, C.; Ochterski, J. W.; Ayala, P. Y.; Morokuma, K.; Voth, G. A.; Salvador, P.; Dannenberg, J. J.; Zakrzewski, V. G.; Dapprich, S.; Daniels, A. D.; Strain, M. C.; Farkas, O.; Malick, D. K.; Rabuck, A. D.; Raghavachari, K.; Foresman, J. B.; Ortiz, J. V.; Cui, Q.; Baboul, A. G.; Clifford, S.; Cioslowski, J.; Stefanov, B. B.; Liu, G.; Liashenko, A.; Piskorz, P.; Komaromi, I.; Martin, R. L.; Fox, D. J.; Keith, T.; Al-Laham, M. A.; Peng, C. Y.; Nanayakkara, A.; Challacombe, M.; Gill, P. M. W.; Johnson, B.; Chen, W.; Wong, M. W.; Gonzalez, C.; Pople, J. A. *Gaussian 03*, revision B.05; Gaussian, Inc.: Pittsburgh, PA, 2003.
(34) Frisch, M. J.; Trucks, G. W.; Schlegel, H. B.; Scuseria, G. E.; Robb, M. A.; Cheeseman, J. R.; Zakrzewski, V. G.; Montgomery, J. A., Jr.; Stratmann, R. E.; Burant, J. C.; Dapprich, S.; Millam, J. M.; Daniels, A. D.; Kudin, K. N.; Strain, M. C.; Farkas, O.; Tomasi, J.; Barone, V.; Cossi, M.; Cammi, R.; Mennucci, B.; Pomelli, C.; Adamo, C.; Clifford, S.; Ochterski, J.; Petersson, G. A.; Ayala, P. Y.; Cui, Q.; Morokuma, K.; Malick, D. K.; Rabuck, A. D.; Raghavachari, K.; Foresman, J. B.; Cioslowski, J.; Ortiz, J. V.; Baboul, A. G.; Stefanov, B. B.; Liu, G.; Liashenko, A.; Piskorz, P.; Komaromi, I.; Gomperts, R.; Martin, R. L.; Fox, D. J.; Keith, T.; Al-Laham, M. A.; Peng, C. Y.; Nanayakkara, A.; Gonzalez, C.; Challacombe, M.; Gill, P. M. W.; Johnson, B.; Chen, W.; Wong, M. W.; Andres, J. L.; Gonzalez, C.; Head-Gordon, M.; Replogle, E. S.; Pople, J. A. *Gaussian 98*, revision A.11; Gaussian, Inc.: Pittsburgh, PA, 1998.